the photolysis of water. 1,2-Dichloroethane, 1,1,2-trichloroethane, 1,1,2,2-tetrachloroethane and chloride ion were produced as major products. Probable reaction mechanisms for the photochemical reaction were presented in Scheme 1.

The fact that 1,2-dichloroethane was the predominant product among the chlorinated organic products implies that the reaction producing $\dot{C}H_2Cl$ radical occurs at a faster rate than that producing $\dot{C}HCl_2$ radical by attack of H and $\dot{O}H$ radicals. With increasing the concentration of oxygen, while the formation of the chlorinated organic products diminished, the formation of chloride ion increased. This is because the primary radicals, formed during the photolysis of aqueous dichloromethane, combined competitively with oxygen. In particular, chloromethylperoxide radicals such as $CHCl_2O\dot{O}$ and $CH_2ClO\dot{O}$, which were produced by combination of oxygen either with $\dot{C}HCl_2$ radical or with $\dot{C}H_2Cl$ radical, increased the formation of chloride ion.

Acknowledgment. We thank Prof. N. Getoff in the University of Vienna, Austria for helpful discussions. KBSI (Korea Basic Science Institute) is acknowledged for the use of HP 5890II GC and 5988 MS spectroscopy.

References

1. Majer, J. R.; Simons, J. P. In *Advances in Photochemistry*, Vol. II: *Photochemical Processes in Halogenated Compounds*; Noyes, W. A., Jr., Hammond, G. S., Pitts, J. N., Jr., Eds.; John Wiley & Sons, Inc.: New York, 1964; p 137, and references therein.
2. Shold, D. M.; Rebbert, R. E. *J. Photochem.* **1978**, *9*, 499.
3. Abadie, M. J. M. *Radiat. Phys. Chem.* **1982**, *19*, 63.
4. Stoessev, R.; Pritze, B.; Abraham, W.; Dreher, B.; Kreysig, D. *J. Prakt. Chem.* **1985**, *327*, 310.
5. Ogita, T.; Hatta, H.; Nishimoto, S. I. *Nippon Kagaku Kaishi* **1985**, *5*, 930.
6. Pacakova, V.; Vojtechova, H.; Coufal, P. *Chromatographia* **1985**, *25*, 621
7. Begishev, I. R.; Belikev, A. K.; Nechitailo, V. G. *Fiz. Goreniya Vzryva* **1991**, *27*, 21.
8. Getoff, N. *Radiat. Phys. Chem.* **1991**, *37*, 673.
9. Halmann, M.; Hunt, A. J.; Spath, D. *Sol. Energy Matter. Sol. Cells* **1992**, *26*, 1.
10. Su, M. C.; Lim, K. P.; Michael, J. V.; Hranisavtjevic, J.; Fontijn, A.; Xun Y. M. *J. Phys. Chem.* **1994**, *98*, 8411.
11. Park, H. R.; Kim, H. J.; Sung, A. Y. *Bull. Korean Chem. Soc.* **1996**, *17*, 798.
12. Florence, T. M.; Farra, Y. J. *Anal. Chim. Acta.* **1971**, *54*, 373.
13. Wolfe, W. C. *J. Anal. Chem.* **1962**, *34*, 1328.
14. Weeks, J. L.; Meaburn, G. M. A. C.; Gordon, S. *Radiat. Res.* **1963**, *19*, 559.
15. Getoff, N. *Monatsheft Chemie* **1968**, *99*, 136.
16. Tomas, J. K. *Int. J. Appl. Radiat. Isotopes* **1965**, *16*, 451.
17. Willson, R. L. *J. Chem. Soc., Faraday Trans* **1971**, *67*, 3008.
18. Calvert, J. G.; Pitts, J. N., Jr. *Photochemistry*; John Wiley & Sons, Inc.: New York, 1967; p 447.
19. Asmus, K. D.; Bahnemann, D.; Krichler, K.; Lal, M.; Moenig, J. *Life Chem.* **1985**, *3*, 1.
20. Catoire, V.; Lesclaux, R.; Lightfoot, P. V.; Rayez, M. T. *J. Phys. Chem.* **1994**, *98*, 2889.
21. Getoff, N.; Prucha, M. *Z. Naturforsch.* **1983**, *38a*, 589.

Monte Carlo Simulation on the Adsorption Properties of Methane in Zeolite L

Sung-Doo Moon*, and Yoshimori Miyano*

Department of Chemistry, Pukyong National University, Pusan 608-737, Korea
**Department of Chemical Technology, College of Science and Industrial Technoloy, Kurashiki University of Science and the Arts, Okayama 712, Japan*
Received October 10, 1996

The adsorption of methane in K^+ ion exchanged zeolite L has been studied using grand canonical ensemble Monte Carlo simulation. Average number of molecules per unit cell, number density of molecules in zeolite, distribution of molecules per unit cell, average potential per sorbate molecule, and isosteric heats of adsorption were calculated, and these results were compared with experimental results. The simulation results agreed fairly well with experimental ones. All methane molecules were located in the main channel, and the average potential of sorbate molecule was almost constant regardless of average number of molecules per unit cell and the amounts sorbed in zeolite.

Introduction

Grand canonical ensemble Monte Carlo (GCMC) simulation has been used to investigate adsorption in zeolites. Thermodynamic adsorption properties of hard sphere,[1] xenon,[2,3] methane[3] in zeolite X and Y have been reported.

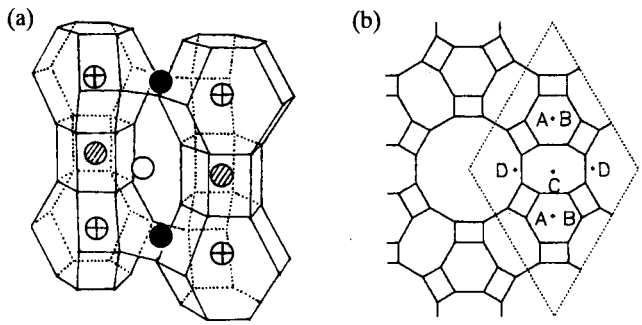

Figure 1. (a) Section of the framework of zeolite L with the different cation sites: site *A* ●; site *B* ⊕; site *C* ●; site *D* ○. (b) Projection of the framework of zeolite L parallel to *c* axis, showing the main channel circumscribed by twelve-membered rings. The labelled positions refer to cation sites in zeolite.

Theodorou and coworkers[4] have calculated adsorption isotherms and isosteric heats of adsorption for alkanes in silicalite, and have also studied[5] on benzene and p-xylene in silicalite. They used new GCMC techniques in which insertion attempts were biased toward the most favorable region of the zeolite pore space. Recently, Smit and coworkers[6] designed the configurational-bias Monte Carlo method to simulate chain molecule, and have used this technique to study the adsorption of n-alkanes in the silicalite and mordenite. These techniques have shown to improve in the efficiency of simulations compared to normal GCMC calculation.

Zeolite[7] L is hexagonal with unit cell dimension a=1.84 nm and c=0.752 nm, and composed of alternating cancrinate cages and hexagonal prisms arranged in connected columns (Figure 1a). This gives rise to the main channel, which is circumscribed by twelve-membered rings along the crystallographic c axis as shown in Figure 1b. The main channel cannot be blocked by simple stacking faults. In fully hydrated form, zeolite has four different sets of cation sites, *A*, *B*, *C*, and *D* sites. *D* sites are near the wall of the main channel and contain those cations which are most likely to be exchangeable at room temperature. Cations in these sites are coordinated to sorbate molecules.

In this paper, the adsorption thermodynamics was studied for methane in dehydrated K^+ ion exchanged zeolite L (K-L) using GCMC calculation. Average number of molecules per unit cell, number density of molecules in zeolite, distribution of molecules per unit cell, average potential per molecule, and isosteric heats of adsorption were calculated. Also these results were compared with experimental ones.

Model and Potential

Potential calculations were carried out using a simplified structural model of dehydated K-L lattice. The unit cell formula of dehydrated K-L is $K_9Al_9Si_{27}O_{72}$. The bond angles and lengths were obtained from X-ray data.[7] For simplicity of calculations the occupancies of cation sites were adjusted as shown in Table 1. Cations having occupancies of 0.5 were alternately placed at the corresponding *A* and *D* sites, and were located at the farthest sites from neighboring cations due to repulsion of cation-cation interaction. Zero

Table 1. Occupancy factor of cation site in ref. 7 (column A) and adjusted occupancy factor used for the present study (column B)

Site	A		B	
	Cation	Fractional occupancy factor	Cation	Fractional occupancy factor
A	Na,K	0.7	K	0.5
B	K	1.0	K	1.0
C	K	0.9	K	1.0
D	Na	0.6	K	0.5

Table 2. Parameters used in calculating potentials (r_i: ionic or atomic radius, k: Boltzmann constant)

ion, atom and molecule	r_i (nm)	σ (nm)	ε/k (K)	$\alpha \cdot 10^{24}$ (cm^3)	n
K^+	0.133[a]	-	-	0.84[a]	17.3[b]
O	0.152[c]	-	-	0.85[c]	8.8[b]
CH_4	-	0.401[d]	142.87[d]	2.62[e]	-

[a] ref. 10, [b] ref. 11, [c] ref. 12, [d] ref. 13, [e] ref. 14

charge was ascribed to Si and Al atoms. A charge equal to +1 was attributed to each K^+ ion. The compensating negative charge was assumed to be distributed uniformly overall oxygen atoms. Consequently a charge of -0.125 was attributed to each oxygen atom. The Si and Al atoms were not directly included in the calculations. This approximation[8] seems justified because Si and Al atoms are completely screened by oxygen atoms, and their polarizabilities are very small, and correspondingly their contribution to the energy of dispersion interaction is negligible. We used the positions[7] of cations in hydrated K-L because those in dehydrated K-L have not been reported yet. The positions of cations and oxygen atoms of zeolite lattice were fixed throughout the calculation because nonpolar sorbate like methane changes little the zeolite structure. Methane molecule was considered as an effective sphere.

The potential between sorbate molecules was calculated using the cut and shifted Lennard-Jones potential,[3]

$$\phi_{ss} = \begin{cases} A_s/r^{12} - B_s/r^6 - \phi_s(r_c), & r < r_c \\ 0 & r \geq r_c \end{cases} \quad (1)$$

where r is the intermolecular distance, subscript s denotes sorbate molecule, and r_c is the cut-off distance. The constant A_s and B_s are given by

$$A_s = 4\varepsilon_s \sigma_s^{12}, \quad B_s = 4\varepsilon_s \sigma_s^6 \quad (2)$$

where ε_s and σ_s are the potential parameters of sorbate molecule (Table 2). For the sorbate-sorbate interactions conventional periodic boundary conditions were applied in all directions. The simulation box consisted of 3 unit cells connected along crystallographic c axis, and r_c was taken as 3.5 σ_s.

The potential between sorbate molecule and zeolite can be represented by the following expression;

$$\phi_{sz} = \sum_i (A_{sz(i)}/r_i^{12} - B_{sz(i)}/r_i^6) - 1/2\alpha_s E^2 \quad (3)$$

where r_i is the distance between molecule and the ith atom of zeolite, α_s and E are polarizability of sorbate molecule and the intensity[8] of electrostatic field at the position of sorbate molecule, respectively. $A_{sz(i)}$ and $B_{sz(i)}$ are the repulsion constant and dispersion constant of the interaction between sorbate molecule and the ith atom of zeolite, respectively. $B_{sz(i)}$ was calculated from $B_{sz(i)}=\sqrt{B_s B_{z(i)}}$. $B_{z(i)}$ was determined by the Slater-Kirkwood formula,[9]

$$B_{z(i)}=\frac{3eh}{8\pi\sqrt{m_e}}\frac{\alpha_{z(i)}^2}{(\alpha_{z(i)}/n_{z(i)})^{0.5}} \tag{4}$$

where e is the electron charge, h is Planck constant, m_e is the electron rest mass. $\alpha_{z(i)}$ and $n_{z(i)}$ are polarizability and the effective number of the outer-shell electrons of the ith atom of zeolite, respectively. $A_{sz(i)}$ was calculated[8] from the condition of the minimum of the potential at the equilibrium distance d_0.

$$A_{sz(i)}=1/2d_0^6[B_{sz(i)}+1/3\alpha_s\eta_{z(i)}^2 d_0^2] \tag{5}$$

where $\eta_{z(i)}$ is the charge of the ith atom of zeolite. It was assumed that d_0 is equal to the sum of ionic or atomic radius in zeolite lattice and a half of equilibrium distance between molecules, $2^{1/6}\sigma_s$. The parameters for calculation are in Table 2.

In general, a pair potential with a spherical cutoff is used to reduce the computing time in computer simulations. In this case, it becomes necessary to correct the results of simulations to compensate for the missing long-range part of the potential. For asymmetric systems like molecules in zeolite, however, it is difficult to estimate the long-range contributions to the results of simulations. To take into account the long-range contributions, a zeolite which consists of 254 unit cells was used in this work. This zeolite was electrically neutral, and a simulation box consisting of 3 unit cells was placed at the center of the zeolite. ϕ_{sz} was calculated by a full image convention. This implies that interactions between a sorbate molecule in simulation box and all atoms of zeolite in the 254 unit cells are taken into account in the calculation of ϕ_{sz}. To verify that the zeolite used in this work was large enough, we calculated ϕ_{sz} at arbitrary point in the simulation box and compared with ϕ_{sz} at the same point in a smaller zeolite which consists of 96 unit cells. We found that ϕ_{sz} in the former zeolite was less by an average of 0.1 percent than ϕ_{sz} in the latter one at test points of about 2×10^5.

To reduce the calculation time of ϕ_{sz} the following simplification was introduced. Unit cell in the simulation box was divided into a large number of cells. ϕ_{sz} was calculated at the center of each divided cell and was stored. The ϕ_{sz} of a molecule placed in a certain divided cell was assumed to be that one calculated at the center of the divided cell. Volume of the divided cell was about 4.3×10^{-6} nm.[3] To check if this volume was small enough or not, the method was applied to the calculation of the thermodynamic properties of adsorption and the results were compared with those obtained for smaller volume of the cell. Practically identical results were obtained.

An effective potential. To get an accurate potential between sorbate molecule and zeolite lattice, the effective potential represented by $\phi_{eff}=\beta\phi_{sz}$ was used in this work.

β was introduced in order to refine ϕ_{sz}, and the value was determined from fitting to the experimental data[15] of isosteric heats of adsorption at very low coverages, q_0. It can be shown that[3]

$$q_0=kT-\frac{kT^2}{V_1}\left(\frac{\partial V_1}{\partial T}\right) \tag{6}$$

where k is Boltzmann constant, and T is absolute temperature. V_1 is the configuration integral and was obtained by an ensemble average[16];

$$V_1=\upsilon<\exp(-\phi_{sz}(r))/kT)> \tag{7}$$

where υ is the volume of simulation box. $\phi_{sz}(r)$ is the potential of a sorbate molecule located at r. β was varied[3] until V_1 by Monte Carlo simulation led to the experimental value of q_0. The value of β was 0.9 for methane.

The discrepancy between ϕ_{eff} and ϕ_{sz} results mainly from two factors. One of them is that K^+ ion positions of D site were assumed to be those in fully hydrated K-L. K^+ ions of D site directly coordinate to sorbate molecules. The interaction between K^+ ion and water molecules is so strong that this cation should be considerably migrated. The other reason is that a charge of K^+ ion in zeolite lattice was assumed to be +1. Several authors[17] have shown that a charge of +1 on univalent cation in zeolite lattice is rather overestimated.

GCMC calculation. We used the GCMC method of Adams[18] in principle. The simulations were performed in cycles, where each cycle consisted of displacement steps and molecule insertion/deletion step. In the displacement steps, every molecule in turn in simulation box was moved by adding random values to the position of molecule. The maximum displacement was adjusted to give an average acceptance ratio of 50 percent. The displacement steps followed closely the procedue given by Miyano.[19]

After the displacement steps, molecule insertion/deletion step was attempted. It was first decided at random and with equal probability whether to attempt to insert a molecule or to delete an existing one. When insertion was attempted, a molecule was inserted into the simulation box at a randomly chosen position. This attempt was accepted with probability

$$P_i=\min[1,\ \exp(G-\Delta E/kT)/(M+1)] \tag{8}$$

where ΔE is the difference in potential between the old and new configurations, M is the number of molecules in the simulation box, and $G=\mu'/kT+\ln<M>$. μ' is the excess chemical potential, and $<M>$ is the average number of molecules in simulation box. The parameter G is fixed at the beginning of the calculation. The value of μ' is obtained from the imposed value of G once $<M>$ is determined. When deletion was attempted, a molecule was randomly selected to be deleted, and deletion was accepted with probability

$$P_d=\min[1,\ M\exp(-G-\Delta E/kT)] \tag{9}$$

The pressure of the bulk fluid corresponding to a given value of chemical potential was estimated numerically using the following equation.[20]

$$\mu=\ln(\Lambda^3 p/kT)+\int_0^p(\overline{V}-\overline{V}_{id})\,dp \tag{10}$$

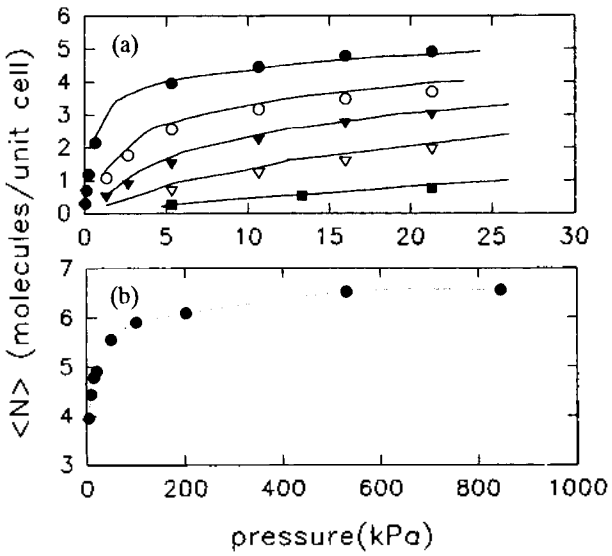

Figure 2. Average number of methane molecules per unit cell <N> as a function of pressure. ●, ○, ▼, ▽, and ■ are GCMC results at 155.8 K, 178.2 K, 192.4 K, 211.6 K, and 243 K, respectively ; — experimental results.[15]

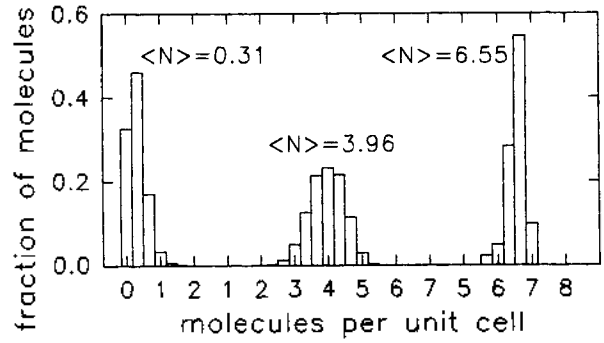

Figure 3. Distribution of methane molecules per unit cell at 155.8 K.

where μ is chemical potential, p is pressure, Λ is the thermal de Broglie wavelength. $\overline{V}$ and $\overline{V}_{id}$ are molar volumes of real and ideal gas, respectively. The value of p at $\overline{V}$ was obtained from the MBWR equation.[21]

The initial configuration[3] was generated by inserting molecules one at a time into the simulation box. Each insertion was only accepted if the total potential of the system resulting from the insertion was less than zero. 5×10^4 GCMC cycles were discarded before 2×10^5 GCMC cycles for equilibrium were performed.

Results and Discussion

Figure 2a shows simulation results for methane in K-L along with experimental results[15] of Barrer *et al.*, and Figure 2b shows only simulation results at high pressure. Here <N> is the average number of molecules per unit cell. Good agreement between the calculated results and the experimental values is seen in Figure 2a. Figure 2b shows that the saturation capacity calculated at 155.8 K is 6.55 molecules per unit cell, which is greater by 0.45 molecule per unit cell than its experimental one.[15]

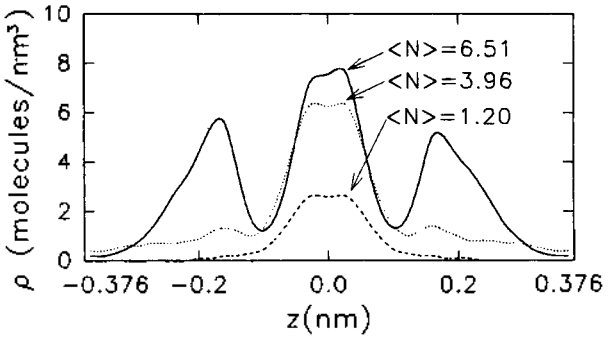

Figure 4. Number density of methane molecules ρ as a function of z coordinate at 155.8 K.

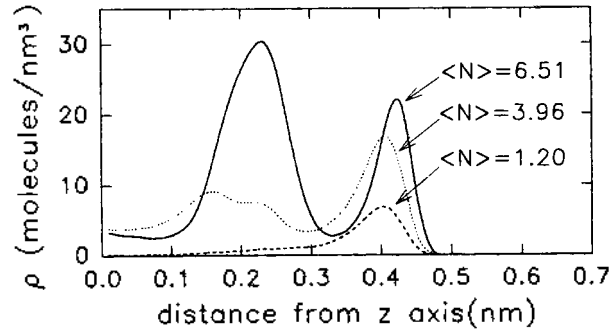

Figure 5. Number density of methane molecules ρ as a function of the distance from z axis at 155.8 K.

Figure 3 presents the distribution of molecules per unit cell at 155.8 K. The distribution of molecules at <N> of 3.96 is broad and symmetric around the most probable occupancy. Whereas the distribution of molecules at <N> of 6.55 is somewhat narrow, which means that more than 7 molecules cannot take in the unit cell. Wood[2] explained this geometric packing effect in their study on the small cavity of zeolite faujasite.

Figure 4 shows number density of methane molecules ρ as a function of z coordinate at 155.8 K, in which the sorbate molecules are distributed symmetrically due to a high degree of symmetry of zeolite framework. Here the origin of z coordinate was taken as the center of cavity which forms the main channel as shown in Figure 1, and z axis was taken along the crystallographic c axis.

Figure 4 obviously indicates most of the sorbate molecules are located in a small region involving z coordinate of zero at <N> of 1.20. The peak heights at z coordinate of zero increase rapidly below <N> of 3.96, whereas those at z coordinates of −0.17 and 0.17nm increase very rapidly above <N> of 3.96. This means that molecules fill preferentially the region between cation of D site and the center of the cavity, and then fill the region between the center of cavity and the intersection of twelve-membered rings which correspond to z coordinates of −0.376 and 0.376 nm.

Number density of molecules ρ in the main channel as a function of the distance from z axis at 155.8 K is presented in Figure 5. Only a simple peak is observed at <N> of 1.20. This peak appears due to molecules adsorbed on sites of the minimum ϕ_{eff}, which lies close to the wall of the main channel. Above <N> of 3.96 additional peaks appear at about 0.2

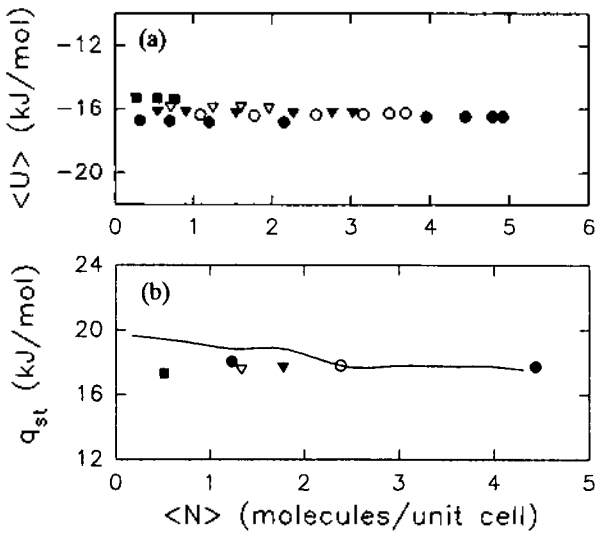

Figure 6. (a) average potential of methane molecule <U> per unit cell, and (b) isosteric heats q_{st} of adsorption as a function of <N>. ●, ○, ▼, ▽, and ■ are GCMC results at 155.8 K, 178.2 K, 192.4 K, 211.6 K, and 243 K, respectively; ——— experimental results.[15]

nm from z axis, and increase rapidly as <N> increases.

From Figure 4 and 5, we suggest that at low loading most of molecules occupy the sites of the minimum ϕ_{eff}, and at medium loading molecules also fill the region of the minimum ϕ_{eff} and simultaneously begin to fill the regions which are less energically favorable, and at high loading mainly the latter regions are filled. However Figure 6a shows that the difference in the average potential of molecule between these two regions are not large. That is, the average potential of the sorbate molecule <U> is almost independent of average number of molecules per unit cell. This is due to that although sorbate molecules are placed in the region which are less favorable of ϕ_{eff} at high loading they can interact with more neighboring molecules. The region near the twelve-membered rings with free diameter[7] of 0.74 nm is large enough to accommodate methane molecules. However there is almost no adsorption in these regions.

If the bulk gas phase is ideal, isosteric heats[5] q_{st} can be calculated as following;

$$q_{st} = RT - \left(\frac{\partial <U>}{\partial <N>}\right)_T \tag{11}$$

where R is gas constant. Since at low pressure methane gas is assumed to be ideal gas, q_{st} is calculated easily from <U> given in Figure 6a.

Figure 6b shows that the calculated q_{st} is almost equal to 17.8 kJ/mol for all <N>, and is constant regardless of temperature. The experimental value[15] of q_{st} also isn't related to temperature, and slowly decreases as <N> increases.

References

1. Sato, J. L.; Myers, A. L. *Mol. Phys.* **1981**, *42*, 971.
2. Woods, G. B.; Panagiotopoulos, A. Z.; Rowlinson, J. S. *Mol. Phys.* **1988**, *63*, 49.
3. Woods, G. B.; Rowlinson, J. S. *J. Chem. Soc., Faraday Trans. 2* **1989**, *85*, 765.
4. June, R. L.; Bell, A. T.; Theodorou, D. N. *J. Phys. Chem.* **1990**, *94*, 1508.
5. Snurr, R. Q.; Bell, A. T.; Theodorou, D. N. *J. Phys. Chem.* **1993**, *97*, 13742.
6. Smit, B.; Siepmann, J. I. *J. Phys. Chem.* **1994**, *98*, 8442.
7. Barrer, R. M.; Villiger, H. Z. *Krist.* **1969**, *128*, 352.
8. Bezus, A. G.; Kiselev, A. V.; Lopatkin, A. A.; Du, P. Q. *J. Chem. Soc., Faraday Trans. 2* **1978**, *74*, 367.
9. Dunfield, L. G.; Burgess, A. W.; Scheraga, H. A. *J. Phys. Chem.* **1978**, *82*, 2609.
10. Nitta, M.; Ogawa, K.; Aomura, K. *J. Phys. Chem.* **1978**, *82*, 1655.
11. Scott, R. A.; Scheraga, H. A. *J. Chem. Phys.* **1965**, *42*, 2209.
12. Kiselev, A. V.; Lopatkin, A. A.; Shulga, A. A. *Zeolites* **1985**, *5*, 261.
13. Reed, T. M.; Gubbins, K. E. In *Applied Statistical Mechanics*; McGraw-Hill, 1973; p 115.
14. Derouane, E. G. *Chem. Phys. Letters* **1987**, *142*, 200.
15. Barrer, R. M.; Lee, J. A. *Surface Sci.* **1968**, *12*, 341.
16. Berne, B. J. In *Statistical Mechanics(part A)*; Plenum Press: New York, 1977; p 171.
17. (a) Morishige, K.: Kittaka, S.; Ihara, S. *J. Chem. Soc., Faraday Trans. 1* **1985**, *81*, 2525. (b) Nivarthi, S. S.; Van Tassel, P. R.; Davis, H. T.; McCormick, A. V. *Zeolites* **1995**, *15*, 40. (c) Kim, J. S.; Jeong, R. H.; Park, S. H.; Ahn, B. J.; No, K. T. *J. Phys. Chem.* **1996**, *100*, 7586.
18. Adams, D. J. *Mol. Phys.* **1975**, *29*, 307.
19. Miyano, Y. *J. Chem. Eng. Japan* **1989**, *22*, 706.
20. Castellan, G. W. In *Physical Chemistry(3rd Ed.)*; Addison-Wesley, p 215.
21. Nicolas, J. J.; Gubbins, K. E.; Streett, W. B.; Tildesley, D. J. *Mol. Phys.* **1979**, *37*, 1429.